Journal of Power Sources 195 (2010) 4435–4443

Contents lists available at ScienceDirect

Journal of Power Sources

journal homepage: www.elsevier.com/locate/jpowsour

Influence of expander components on the processes at the negative plates of lead-acid cells on high-rate partial-state-of-charge cycling. Part I: Effect of lignosulfonates and $BaSO_4$ on the processes of charge and discharge of negative plates

D. Pavlov*, P. Nikolov, T. Rogachev

Institute of Electrochemistry and Energy Systems, Bulgarian Academy of Sciences, Acad. Georgi Bonchev Street, bl. 10, Sofia 1113, Bulgaria

ARTICLE INFO

Article history:
Received 3 November 2009
Received in revised form
12 November 2009
Accepted 13 November 2009
Available online 20 November 2009

Keywords:
Lead-acid battery
Negative active mass
Expander in lead-acid cells
High-rate partial-state-of-charge
Lignosulfonates in lead-acid battery
Barium sulfate in lead-acid battery

ABSTRACT

This study investigates the influence of the organic expander component (Vanisperse A) and of $BaSO_4$ on the performance of negative lead-acid battery plates on high-rate partial-state-of-charge (HRPSoC) cycling. Batteries operating in the HRPSoC mode should be classified as a separate type of lead-acid batteries. Hence, the additives to the negative plates should differ from the conventional expander composition. It has been established that lignosulfonates are adsorbed onto the lead surface and thus impede the charge processes, which results in impaired reversibility of the charge–discharge processes and hence shorter cycle life on HRPSoC operation, limited by sulfation of the negative plates. $BaSO_4$ exerts the opposite effect: it improves the reversibility of the processes in the HRPSoC mode and hence prolongs the cycle life of the cells. The most pronounced effect of $BaSO_4$ has been registered when it is added in concentration of 1.0 wt.% versus the leady oxide (LO) used for paste preparation. It has also been established that $BaSO_4$ lowers the overpotential of $PbSO_4$ nucleation. The results of the present investigation indicate that $BaSO_4$ affects also the crystallization process of Pb during cell charging. Thus, $BaSO_4$ eventually improves the performance characteristics of lead-acid cells on HRPSoC cycling.

1. Introduction

Conversion of electrical energy into chemical one and vice versa proceeds through electrochemical reactions at the interface solid phase/solution. The reactions at the two types of electrodes in a lead-acid cell generate Pb^{2+} ions which react with H_2SO_4 forming $PbSO_4$. During discharge, a $PbSO_4$ film is formed on the surface of the negative electrode. This film passivates the electrode and hence the capacity and power output of the battery decline substantially. In order to avoid this phenomenon, some additives, generally known as 'expander', are introduced in the negative paste. As a rule, the expander comprises three components: lignosulfonate, $BaSO_4$ and carbon additives.

After the Second World War, when wood separators were replaced by synthetic polymer materials, it was established that negative plates suffered a drastic decrease in capacity during cycling operation, especially at low temperatures. Investigations revealed that this phenomenon resulted from the absence of lignosulfonic acid leached from the wooden separator into the electrolyte. So it became necessary to add lignosulfonates to the negative active mass.

Many researchers have studied the effects of lignosulfonates on lead-acid battery negative plates throughout the years [1–13]. It has been established that lignosulfonates prevent the deposition of a passivating $PbSO_4$ layer on the electrode surface and facilitate the formation of a porous layer built up of individual $PbSO_4$ crystals instead, which results in multifold increase of lead electrode capacity. Recently, Hirai et al. have conducted in situ examinations of the structure of the passivating and of the porous $PbSO_4$ layers [13]. In this paper the authors have also provided an excellent survey of earlier publications on the influence of lignosulfonates on the performance characteristics of lead-acid batteries. They have demonstrated experimentally how lignosulfonates retard the reactions of charge and discharge, but increase the capacity of the negative plates [13].

It is generally assumed that carbon black is introduced in the negative paste mainly to improve the electric conductivity of the negative active mass at the end-of-discharge, when the content of $PbSO_4$ crystals in NAM increases substantially [14–21].

It is also assumed that barium sulfate ($BaSO_4$) acts as a nucleation agent (nucleant) for $PbSO_4$ crystal formation and growth. This function of $BaSO_4$ is a result of the isomorphism between

* Corresponding author. Tel.: +359 2 971 00 83; fax: +359 2 873 15 52.
E-mail addresses: dpavlov@labatscience.com, dinart@kz.orbitel.bg (D. Pavlov).

0378-7753/$ – see front matter © 2009 Elsevier B.V. All rights reserved.
doi:10.1016/j.jpowsour.2009.11.060

$PbSO_4$ and $BaSO_4$ crystals. Hence, $BaSO_4$ ensures uniform distribution of $PbSO_4$ crystals throughout the active mass volume [23–30].

During operation of VRLA batteries under high-rate partial-state-of-charge (HRPSoC) conditions lead sulfate is progressively accumulated in the negative plates as a result of which the cycle life of the batteries is shortened considerably. When these batteries are used in hybrid electric vehicle applications, their charge efficiency is very low. Nakamura et al. [14] and Shiomi et al. [15] have established that addition of carbon black to the negative active material retards substantially the sulfation of the negative plates on HRPSoC cycling. Several hypotheses about the mechanism of action of carbon have been proposed [15–19], which are summarized by Moseley [20].

In an investigation conducted in our laboratory recently we have established that the electrochemical reactions of charge and discharge of the negative plates proceed via a parallel mechanism on the surfaces of both Pb and carbon black particles [21], thus increasing the overall electrochemically active surface of the negative electrode. It could be expected that there would be a competition between the reactions at the two surfaces and their rates will depend on the type and amount of carbons added.

This new hypothesis about the parallel mechanism of charge of the negative plates posed the question about the specific influence of the other two expander components (lignosulfonate and $BaSO_4$) on the processes during HRPSoC operation.

The aim of the present investigation is to elucidate the effect of the organic expander components lignosulfonate (its most widely used representative, the commercial product Vanisperse A) and of $BaSO_4$ on the processes that take place during HRPSoC cycling. The influence of carbon additives on the HRPSoC processes will be discussed in a separate publication to follow as part II of this paper.

The tests are performed using 4.5 Ah cells that are initially 100% saturated with 1.27 sp.gr. H_2SO_4 electrolyte and then lose water during the cycling test, hence the saturation decreases below 96% and the cells start to behave like valve-regulated lead-acid batteries (VRLAB) with an operative closed oxygen cycle.

2. Experimental

2.1. Test lead-acid cells

2.1.1. Negative paste preparation

The negative pastes were prepared using H_2SO_4 (1.4 sp.gr.) and leady oxide (LO) in 4.5 wt.% ratio. The degree of oxidation of the LO was 76%. Barton oxide from battery plant "Monbat", Bulgaria, was used. Paste batches with addition of Vanisperse A alone, in concentration 0.2% or 0.3% versus the weight of the LO, were prepared and used to investigate the effect of the organic expander component VS-A. For the experiments aimed to study the influence of $BaSO_4$, the pastes were prepared with addition of $BaSO_4$ alone in four different concentrations: 0.5, 1.0, 1.5 or 2.0 wt.% versus the LO. A batch of paste with a combination of 0.8% $BaSO_4$ and 0.2% VS-A, without carbon additives, was also prepared for comparison.

The above pastes were used for production of negative plates for the test cells. The pasted plates were cured under the following conditions: 48 h at 35 °C and 98% relative humidity, followed by 24 h at 60 °C and 10% relative humidity. All plates were formed in H_2SO_4 (1.06 sp.gr.) for 18 h, employing a formation algorithm developed in this laboratory. The formation process was completed with twice higher quantity of electricity than the theoretical capacity of the plates. After formation, samples of the negative active material were characterized by XRD, chemical analysis and SEM examinations.

Design of test cell

- 2 V / 4.5 Ah test cell
- 2 negative plates
- 3 positive plates (oversized)
- AGM separator: 3 mm thick
- separator compression: 20%
- 75 ml 1.27 sp. gr. H_2SO_4

Measured cell parameters

- initial C_{20} capacity tests
- Peukert dependence
- HRPSoC cycling

Fig. 1. Photograph of the 2 V/4.5 Ah test cell.

2.1.2. Test cell design

The influence of VS-A and $BaSO_4$ additives on the performance of lead-acid cells was investigated using 4.5 Ah cells with two negative and three positive plates per cell. The test cell design is presented in Fig. 1 and its characteristics are summarized in Table 1.

The performance parameters of the cells were limited by the negative plates. Small sized plates were used to rule out the influence of plate size on cell performance as well as of electrolyte stratification in the cell. AGM separators (H&V, USA) with a thickness of 3 mm (425 g m^{-2}) were used at 20% compression. 75 ml H_2SO_4 solution of 1.27 sp.gr. was poured in the cells (the electrolyte forming a "mirror" over the plates) and the cells were sealed. During the subsequent cycling tests part of the water decomposed, the electrolyte saturation of the cells decreased and they started to operate like VRLA cells with an operative closed oxygen cycle. The rated capacity of the cells at 20 h discharge, C_0, was calculated at 50% utilization of the negative active material.

2.2. Electrical parameters of the test cells

2.2.1. Initial cell capacity

The initial capacity of the cells was determined at a discharge current of $I = C_0/20A$. Each cell was subjected to three subsequent capacity tests at 25 °C.

2.2.2. Peukert dependences

The Peukert dependences were obtained at $C/20$, $C/10$, $C/7$, $C/5$, $C/3$, $1C$ and $2C$ rates. Charging was conducted in two steps: first step $I_{ch} = 0.5C_0A$ to a voltage limit of 2.45 V, and second step $I_{ch} = 0.2C_0A$ to 120% overcharge. The rest period after charge was 30 min. All cell tests were performed using Bitrode testing equipment. From the obtained Peukert curves the $1C$ and $2C$ currents for the HRPSoC cycling tests were determined.

2.2.3. Cycle life test under simulated HRPSoC regime

The effects of lignosulfonate and $BaSO_4$ on cell performance under simulated HRPSoC conditions were evaluated using a simplified profile imitating the micro-hybrid driving mode. This cycling mode has been generally accepted for projects implemented within

Table 1
Test cell design characteristics.

	Negative plate	Positive plate
Grid alloy (wt.%)	Pb–0.04Ca–1.1Sn	Pb–0.04Ca–1.1Sn
Grid thickness (mm)	1.5	1.5
Grid dimensions (mm)	57 × 60	57 × 60
Plates per cell	2	3
Plate thickness (mm)	2.0	2.5

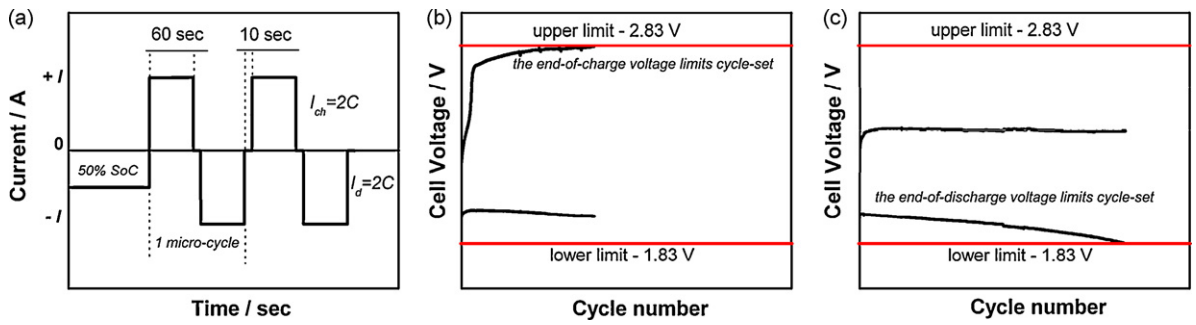

Fig. 2. (a) Current profile of a micro-cycle of the HRPSoC cycling test; (b) the end-of-charge voltage limits the cycle-set of the HRPSoC test; (c) the end-of-discharge voltage limits the cycle-set of the HRPSoC test.

the Advanced Lead-Acid Battery Consortium (ALABC) program. The current profile of the HRPSoC cycling test is presented in Fig. 2.

The first step in this cycling profile was discharge at $I = 1CA$ rate to 50% SoC. After that, the cells were subjected to cycling according to the following schedule: charge at 2*C* rate for 60 s, rest for 10 s, discharge at 2*C* rate for 60 s, rest for 10 s. (*C* is the capacity after 1 h discharge determined from the Peukert dependence.) During these tests the plates were cycled at only 3% depth of discharge within each micro-cycle, starting from 50% SoC. The cell voltage was measured at the end of the charge or discharge pulses and the test was stopped when the cell voltage fell down to 1.83 V or when the upper voltage limit of 2.83 V was reached. The above described cycling steps comprise one cycle-set of the test. The cells were fully re-charged (to 100% SoC) after this cycle-set and their C_{20} capacity was measured. Then the cells were discharged with 1*CA* to 50% SoC and a new cycle-set was conducted. We have assumed conditionally that the cell has reached its end of life when it completes less than 4000 micro-cycles within one cycle-set and/or when its capacity falls below 70% C_0. On completion of the HRPSoC cycle life test the cells were subjected to teardown analysis.

2.3. Model electrodes and experimental set-up

To evaluate the influence of each additive to the negative active mass on the processes during cycling of the negative plates, model electrodes (ME) were used analogous to those developed and employed in earlier investigations of ours [21,31]. The modified design of the model electrode is presented diagrammatically in Fig. 3.

It comprises a Pb–0.1% Ca spine, inserted in a PTFE (Teflon) holder, covered with an AGM separator and pressed with a PTFE ring-cap. This model electrode was used to demonstrate the processes that proceed at the Pb/$PbSO_4$ electrode during charge and discharge (Fig. 3a).

For the experiments aimed to examine the influence of $BaSO_4$ on the charge and discharge processes, a model electrode of the same design was used, but there was a small cavity in the center of the Pb spine which was filled with $BaSO_4$ (Fig. 3b).

Thus, the Pb model electrode demonstrates the charge and discharge processes at the Pb electrode, whereas the (Pb + $BaSO_4$) model electrode illustrates the influence of $BaSO_4$ on these processes.

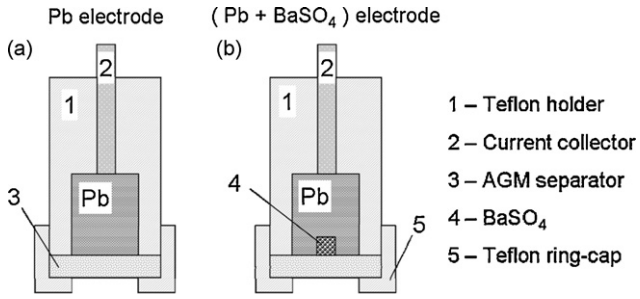

Fig. 3. Model electrode design.

The experiments were carried out in a classical three-electrode cell comprising a ME as working electrode, an $Hg/Hg_2SO_4/H_2SO_4$ reference electrode and a large Pt mesh as counter electrode. All experiments were performed in excess of 1.28 sp.gr. sulfuric acid solution at ambient temperature. Linear sweep voltammetry measurements were conducted. The potential of the working electrode was swept between −0.5 V and −1.3 V at a scan rate of 20 mV s^{-1}.

3. Experimental results and discussion

3.1. Initial capacity of cells with VS-A or $BaSO_4$ added to the negative plates

The rated capacity of the cells, C_0, was calculated at 50% utilization of the negative active mass versus the theoretically calculated quantity of electricity that can be delivered by the lead used for negative plate manufacture. The initial capacity of the cells was determined experientially after 20 h of discharge with $I = C_0/20A$. The obtained results are summarized in Table 2.

All cells have initial capacities higher than the rated value of $C_0 = 4.5$ Ah. After the first initial capacity measurement the cell capacity decreases rapidly with each subsequent capacity test. The highest initial capacity values are measured for the cells with 0.3% VS-A or 1.0% $BaSO_4$ in the negative plates. An interesting finding is

Table 2
Initial C_{20} capacities of cells with different concentrations of VS-A or $BaSO_4$.

Cell	First C_{20} discharge capacity (Ah)	Second C_{20} discharge capacity (Ah)	Third C_{20} discharge capacity (Ah)
0.2% Vanisperse-A	5.90	5.54	5.16
0.3% Vanisperse-A	5.87	5.71	5.44
0.5% $BaSO_4$	5.71	5.39	5.02
1.0% $BaSO_4$	6.30	5.91	5.43
1.5% $BaSO_4$	5.71	5.34	4.93
2.0% $BaSO_4$	5.65	5.24	4.83

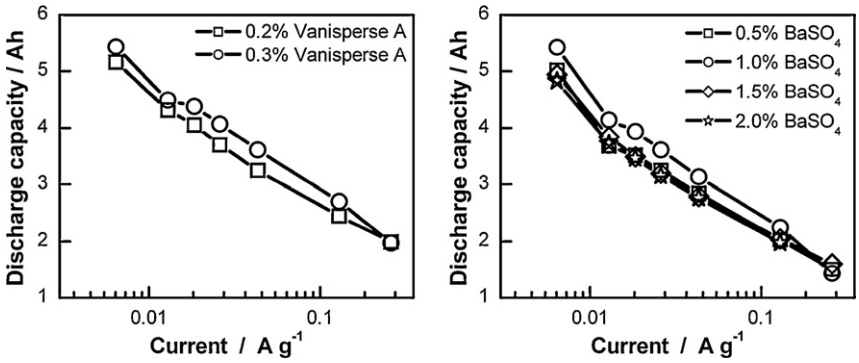

Fig. 4. Peukert dependences for cells with different concentrations of VS-A or $BaSO_4$ in the negative plates.

that the capacity of these cells declines most slowly during the second and third capacity measurements. So it can be expected that these cells will have the best performance characteristics on HRPSoC cycling. The cycling behaviour of all other test cells depends on the type and amount of the additives used.

3.2. Peukert dependences for cells with negative plates containing different amounts of VS-A or $BaSO_4$

Fig. 4 presents the obtained Peukert curves for cells with different loads of VS-A or $BaSO_4$. A comparative analysis of the experimental results indicates that the cells with VS-A have higher capacity than those with $BaSO_4$ at all discharge currents. This difference is most pronounced within the range of medium current densities.

The cell with 0.3% VS-A has higher capacity than the cell with 0.2% VS-A load in the negative plates at all current densities, except for the discharge with 2*CA*.

The capacities of the cells with 0.5, 1.5 or 2.0% $BaSO_4$ are very close in values for all discharge rates. The capacity curve for the cell with 1.0% $BaSO_4$ in the negative plates is shifted to higher values as compared to all other cells. Obviously, this cell has the greatest potential for current generation than the other members of the $BaSO_4$ family.

3.3. Influence of organic expander component on the performance of cells in the HRPSoC cycling duty

3.3.1. Structure of the lead active mass containing VS-A

The structure of the lead (negative) active mass (NAM) comprises: (a) *a skeleton* built-up of large lead particles, which conducts the current to, or collects it from, every part of the NAM volume, and (b) *energetic structure* built-up of a huge number of small lead crystallites grown over the skeleton surface. These crystallites participate in the charge–discharge processes on cycling of the cells [32]. Formation of the energetic structure is influenced by the organic expander component, the lignosulfonate [33].

Fig. 5 shows SEM pictures of samples of the negative active mass containing 0.2% or 0–.3% Vanisperse A.

The image of the NAM sample with 0.2% VS-A load features small lead crystals of the energetic structure which are bonded, individually or in groups, to the surface of the large and well shaped crystals building the skeleton structure. The energetic structure of the NAM sample with 0.3% VS-A comprises numerous small Pb particles interconnected into agglomerates, which have grown over the large crystals of the skeleton structure. And the skeleton structure itself is not so well shaped as in the NAM with 0.2% VS-A. It can be expected that these structural differences will affect the processes during HRPSoC cycling of the cells.

3.3.2. HRPSoC cycling performance of cells with different content of lignosulfonate in NAM

Fig. 6 presents the completed number of cycles and the capacity of the cells within each cycle-set of the HRPSoC test. The cell with 0.2% VS-A completes 3 cycle-sets with a total of 20,600 cycles against 6000 cycles for the cell with 0.3% VS-A. The increased load of Vanisperse from 0.2% to 0.3% reduces substantially the number of completed cycles within one cycle-set. The capacity of both cells declines after each cycle-set, but the two cells have the same capacity despite the different number of completed HRPSoC cycles.

Fig. 7 shows the measured end-of-charge and end-of-discharge voltages for the two cells on cycling.

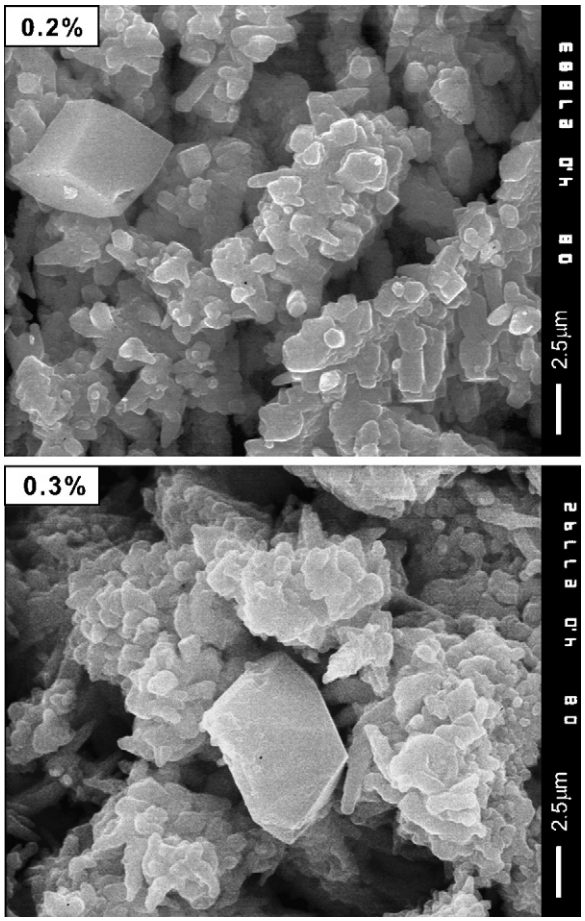

Fig. 5. SEM micrograph of negative active mass (NAM) with 0.2% or 0.3% Vanisperse A.

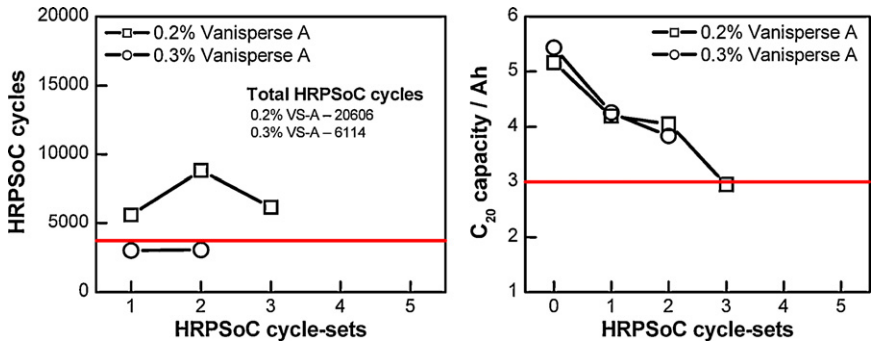

Fig. 6. Completed HRPSoC cycles and C_{20} capacity of the test cells after each cycle-set of the HRPSoC test.

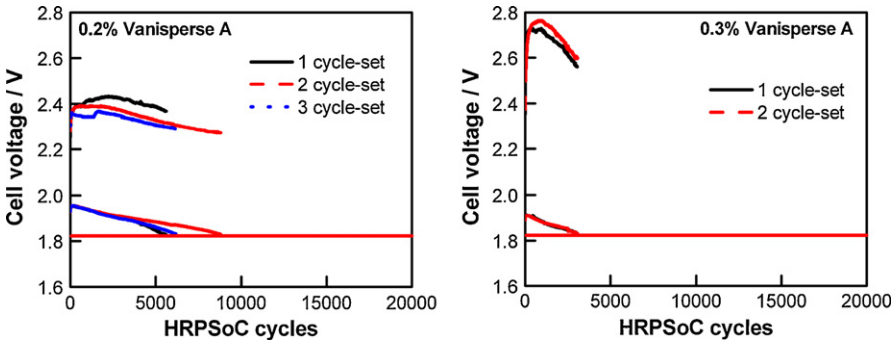

Fig. 7. End-of-charge and end-of-discharge cell voltages on HRPSoC cycling.

The duration of each cycle-set is limited by the end-of-discharge voltage which reaches the lower voltage limit of 1.83 V. These results indicate that the negative plates are heavily sulfated during cycling. The rate of this sulfation process determines the number of completed HRPSoC cycles. The measured charge voltages of the two cells are different. The increased VS-A content leads to an increase of the cell voltage during charge, which is about 2.4 V for the cell with 0.2% VS-A versus 2.75 V for the cell with 0.3% VS-A load. This experimental finding indicates that the organic expander component (lignosulfonate) is adsorbed on the lead surface and impedes considerably the charge process of the negative plates (0.35 V polarization). When the plates contain 0.2% VS-A the latter does not cover the whole lead surface and the charge reaction proceeds on the free electrode surface areas, hence the charge voltage is low. In the plates with 0.3% VS-A, the surface of the negative plates is entirely covered by adsorbed VS-A molecules, causing increased polarization of the negative plates. The charge process is impeded, which results in increased sulfation of the plates and reduces markedly the number of completed cycles within one HRPSoC cycle-set, which is actually observed in Fig. 6.

3.4. Influence of $BaSO_4$ added to the negative paste on cell HRPSoC cycling performance

3.4.1. Structure of $BaSO_4$ and of the negative active mass containing $BaSO_4$

Fig. 8 shows SEM images of $BaSO_4$ particles used as additive to the negative paste for lead-acid batteries. Barium sulfate particles are rounded or egg-shaped with sizes within the range from 0.1 μm to 0.5 μm.

The SEM pictures presented in Fig. 9 feature the structure of NAM with various content of $BaSO_4$.

The sample with 0.5% $BaSO_4$ comprises big lead particles interconnected to form a skeleton. The small particles over the lead skeleton are, probably, $BaSO_4$ particles. The SEM image of NAM with 1.0% $BaSO_4$ features smaller Pb crystals with $BaSO_4$ particles fairly well bonded to them. The Pb active mass structure presented

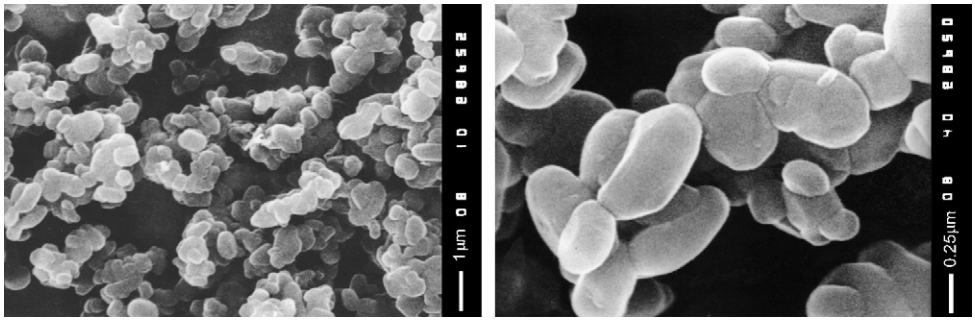

Fig. 8. SEM micrographs of $BaSO_4$ particles used as additive to the negative active mass.

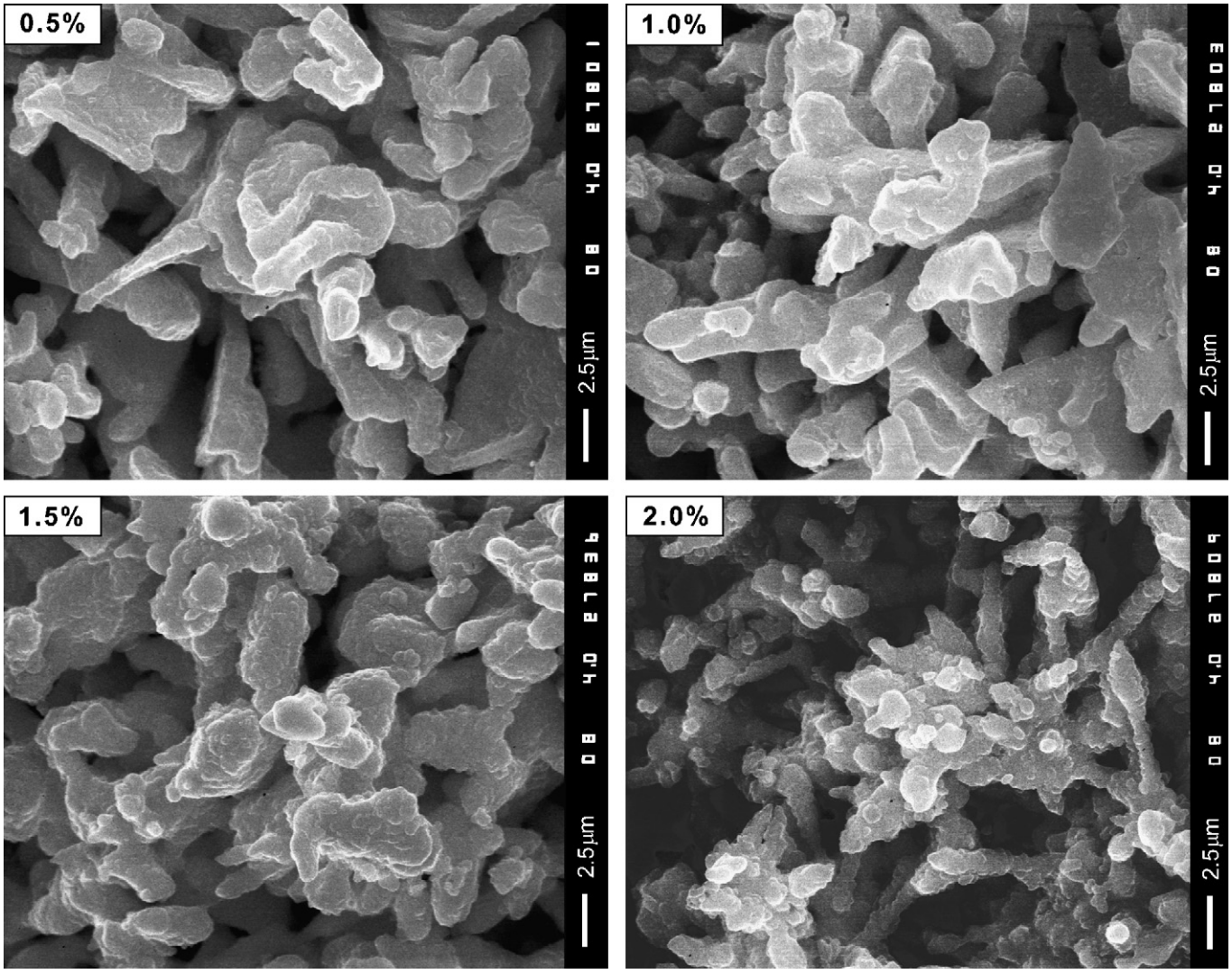

Fig. 9. SEM micrographs of NAM with different content of $BaSO_4$.

in the next two pictures (for 1.5% and 2.0% $BaSO_4$ loading levels) is built-up of smaller Pb particles. The effect of $BaSO_4$ is usually related to its influence on the crystallization processes of $PbSO_4$ [22–29]. The above SEM images, however, indicate that $BaSO_4$ affects also the Pb crystallization processes. An increase of the load of $BaSO_4$ in NAM from 1.0% to 2.0% changes the size of the Pb agglomerates formed by interconnected Pb particles (especially at 2.0% $BaSO_4$ content). How does this indifferent agent ($BaSO_4$) intervene in the crystallization processes of lead remains still an open question.

3.4.2. *Influence of $BaSO_4$ on the cycle life of cells in the HRPSoC duty*

Fig. 10 presents the completed HRPSoC cycles and the capacity of cells with various amounts of $BaSO_4$ in NAM during several HRPSoC cycle-sets.

The cells with 1.0% or 1.5% $BaSO_4$ in NAM complete the greatest number of cycles within each cycle-set, but their capacity declines rapidly to 3.0 Ah, i.e. reach the assumed conditional cycle life limit of 70% of the rated capacity. These cells still complete over 6000

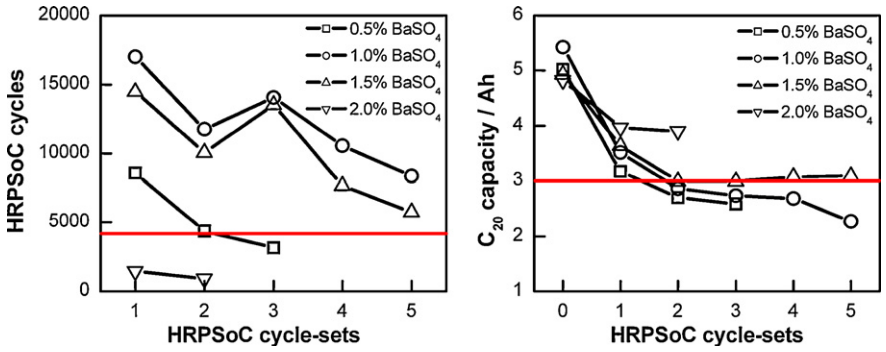

Fig. 10. HRPSoC cycles and C_{20} capacity of cells with different amounts of $BaSO_4$ in NAM for five cycle-sets of the HRPSoC test.

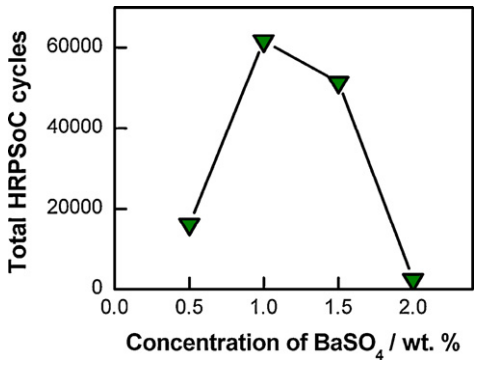

Fig. 11. Total number of completed HRPSoC cycles as a function of $BaSO_4$ content in NAM.

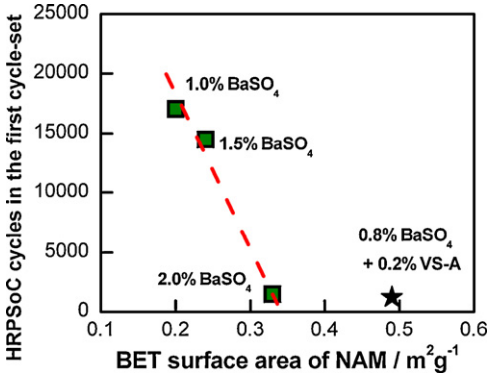

Fig. 12. Completed HRPSoC cycles within the first cycle-set for cells with different amounts of $BaSO_4$ as a function of BET surface area of NAM.

cycles during the 5th cycle-set, which means that they have not yet reached the end of their cycle life according to the assumed HRPSoC life limit.

The cell with 2.0% $BaSO_4$ has the shortest cycle life, but the highest C_{20} capacity after the first and the second cycle-sets. This indicates that the processes that occur on deep discharge (at 20-h rate) and on HRPSoC cycling differ substantially and so do the parameters that limit the cycle life of cells in the two cycling modes. Therefore, the two end-of-cycle life criteria (completed cycles and cell capacity) should be specified for the two cycling duties (HRPSoC or deep-discharge cycling), and appropriate types and amounts of additives to the negative plates should be selected for each operation mode. Hence, depending on the intended cycling application, the batteries should be classified as different battery types.

Fig. 11 shows the total number of completed cycles by cells with different $BaSO_4$ concentration in NAM.

It is interesting to note that the cells with 1.0% or 1.5% $BaSO_4$ have a potential to endure more than 5 cycle-sets without reaching the assumed lower cycle life limit of 4000 micro-cycles per cycle-set. In view of this limit, the longest cycle life is registered for the cell with 1.0% $BaSO_4$ in NAM.

The completed HRPSoC cycles within the first cycle-set for cells with different amounts of $BaSO_4$ are presented in Fig. 12 as a function of BET surface area of NAM.

The overall NAM surface area is a sum of the surfaces of the three components of the negative active mass: Pb, $BaSO_4$, $PbSO_4$.

$$S_{NAM} = S_{Pb} + S_{BaSO4} + S_{PbSO4}$$

The data in Fig. 12 evidence that with increase of the $BaSO_4$ content in NAM the overall NAM surface area increases, too. However, the contribution of the $BaSO_4$ surface is not sufficient to account for the observed increase in NAM surface area. Obviously, the larger BET surface of NAM is partially due to the finer lead structure as illustrated in Fig. 9. Fig. 11 shows that at 1.0% $BaSO_4$ loading level in NAM the cells complete the greatest number of micro-cycles on HRPSoC cycling, i.e. the reversibility of the processes of charge and discharge is the highest in this particular 1 min cycling mode. Probably, at this concentration of $BaSO_4$ in NAM, there is an optimum ratio between the surfaces of Pb and $BaSO_4$ ensuring higher reversibility of the charge–discharge micro-cycles.

The data in Fig. 12 indicate also that negative plates with 0.8% $BaSO_4$ and 0.2% VS-A have considerably larger NAM surface, but complete a very small number of HRPSoC cycles in the first cycle-set. In this case, VS-A influences the crystallization process of Pb during plate formation yielding small Pb crystals thus increasing the overall NAM surface. However, this fine Pb crystal structure is not very stable and it has high ohmic resistance. Besides, VS-A retards the charge processes on cycling. Hence, the rate of negative plate sulfation increases, which is the reason for the smaller number of completes micro-cycles within the first HRPSoC cycle-set.

It follows from all above said that for cycling regimes with mini charge–discharge pulses (1 min) and high currents, the active mass should have a skeleton structure built of thick skeleton branches so as to have low ohmic resistance throughout the volume of NAM and thus to guarantee long cycle life in the HRPSoC duty. Such a structure of the active mass is characterized also by larger pores which facilitate the transport of sulfuric acid in NAM.

3.4.3. *Influence of $BaSO_4$ on the crystallization processes of Pb and $PbSO_4$*

Barium sulfate is isomorphous with $PbSO_4$. Hence, its particles provide nuclei for the growth of $PbSO_4$ crystals. Fig. 13 presents the measured cell voltages of cells with $BaSO_4$ (0.5% or 1.0%) or VS-A (0.2%) at the beginning of discharge.

In the cell with VS-A alone, $PbSO_4$ nuclei have to be formed first which then will grow into $PbSO_4$ crystals. The process of $PbSO_4$ nucleation leads to polarization of the cell by some 90 mV, which is the overpotential of nucleation of the $PbSO_4$ phase, $\Delta\varphi_n$. No such

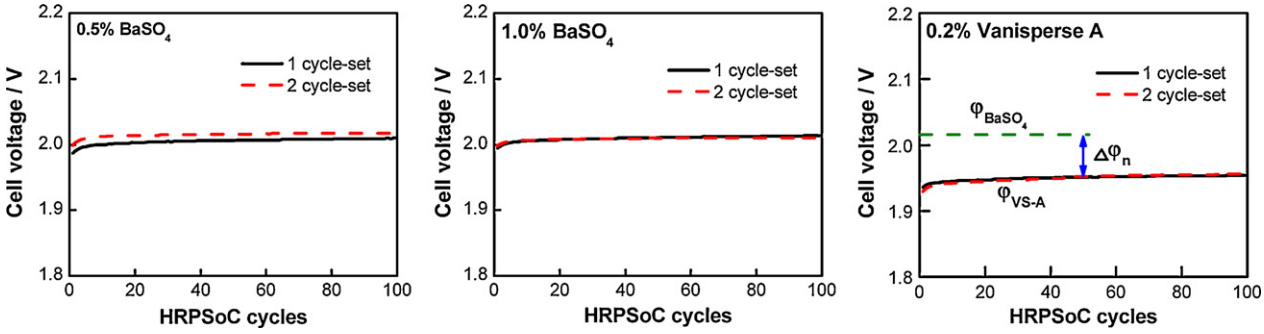

Fig. 13. Discharge voltage of cells with $BaSO_4$ or VS-A during the first 100 micro-cycles. $\Delta\varphi$ is the overvoltage of $PbSO_4$ nucleation.

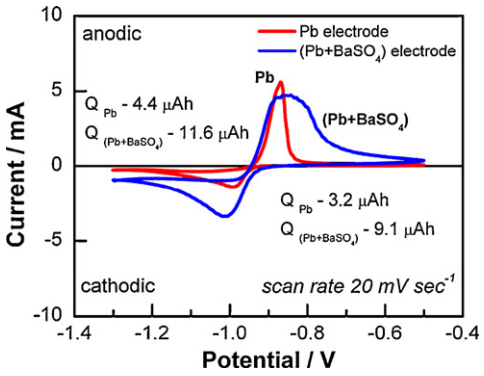

Fig. 14. Voltammograms for Pb and (Pb + $BaSO_4$) electrodes on polarization in the potential range from −0.5 V to −1.3 V vs. Hg/Hg_2SO_4 electrode at a scan rate of 20 mV s^{-1}.

polarization is observed during discharge of the cells with $BaSO_4$, because the latter's particles serve as nuclei onto which $PbSO_4$ crystals precipitate and grow [29]. Hence, $BaSO_4$ reduces the overpotential of $PbSO_4$ nucleation due to the isomorphism between the two compounds.

This is how $BaSO_4$ affects the initial phase of the crystallization process of $PbSO_4$. The question arises as to whether $BaSO_4$ facilitates the crystal growth and the dissolution of $PbSO_4$ crystals on cycling. We followed its effect by linear sweep voltammetry measurements on model Pb and (Pb + $BaSO_4$) electrodes. Voltammetry tests were conducted in the potential range from −0.5 V to −1.3 V vs. Hg/Hg_2SO_4 electrode at a scan rate of 20 mV s^{-1}. The obtained voltammograms are presented in Fig. 14. The quantities of electricity (in μAh) measured at the anodic and cathodic peaks for the two types of electrodes are also given in the figure.

Obviously, $BaSO_4$, though localized as a separate phase in the center of the lead electrode, increases the rate of both the anodic and cathodic reactions. Thus, during the anodic reaction of oxidation of Pb and formation of $PbSO_4$ the ratio between the quantities of electricity $Q_{(Pb+BaSO4)}$ and Q_{Pb} is equal to 2.64. This indicates that $BaSO_4$ exerts a strong influence on the processes of $PbSO_4$ crystallization by attracting the Pb^{2+} ions released by the oxidation of Pb and thus retarding the formation of a passivating $PbSO_4$ layer on the Pb surface which would impede the anodic reaction. It is true that the $BaSO_4$ volume in the cavity is porous and the pores are filled with electrolyte. This would increase to some extent the Pb surface which is contact with $BaSO_4$, but it could hardly be expected that this increase would be by a factor of 2.64. Moreover, the resistance to the current flowing through the pores would be high and hence this current and the current from the side surfaces of the $BaSO_4$ volume will have but a small contribution to the overall electric current.

During the cathodic polarization scan, the ratio between the quantities of electricity $Q_{(Pb+BaSO4)}$ and Q_{Pb} is equal to 2.84. Obviously, the cathodic reaction of $PbSO_4$ reduction to Pb involves also the $PbSO_4$ crystals precipitated on the surface of the $BaSO_4$ particles.

Fig. 15 represents schematically the exchange of Pb^{2+} ions between the Pb and $BaSO_4$ parts of the (Pb + $BaSO_4$) electrode during the reactions of Pb oxidation and $PbSO_4$ reduction.

The surface area of the Pb electrode base is 0.38 cm^2. The outer surface area of the cavity filled with $BaSO_4$ is 0.14 cm^2, i.e. the Pb surface is 2.7 times larger than the $BaSO_4$ contact surface. Yet, the volume of $BaSO_4$ filled in the cavity increases by a factor of 2.6 the quantity of electricity flowing through the (Pb + $BaSO_4$) model electrode during the anodic process of Pb oxidation, and by a factor of 2.8 the electricity during the cathodic process of $PbSO_4$ reduction, as compared to the Pb model electrode. This means that the $BaSO_4$

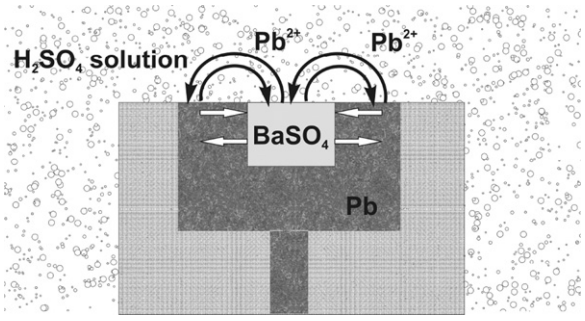

Fig. 15. Schematic representation of the exchange of Pb^{2+} ions between the Pb and $PbSO_4$ parts of the (Pb + $BaSO_4$) electrode during the reactions of Pb oxidation and $PbSO_4$ reduction.

phase, though confined in a separate volume, affects the crystallization processes of $PbSO_4$, and also of Pb, as evidenced by the SEM images in Fig. 9. It is interesting to disclose the mechanism by which $BaSO_4$ exerts this influence.

4. Conclusions

Batteries operating in the HRPSoC cycling duty should be classified as a separate type of lead-acid batteries designed for short charges and discharges with high currents. Additives to the negative plates of such batteries should differ in type and amount from those introduced in conventional SLI, traction and stationary batteries.

Lignosulfonates are adsorbed on the lead surface and impede the charge processes, thus eventually shortening the cycle life of the cells in the HRPSoC duty.

$BaSO_4$, added alone to the negative paste in an amount of 1.0 wt.% vs. the LO, prolongs substantially the life of the cells subjected to HRPSoC cycling. It facilitates the Pb crystallization process and the dissolution of $PbSO_4$, and thus improves the reversibility of the charge–discharge processes. 1.0% $BaSO_4$ loading level in the paste ensures optimum ratio between the surface areas of Pb and $BaSO_4$ in NAM for the processes during the short-term charge and discharge cycles with high currents to proceed, and hence yields the best cycle life performance of the cells in the HRPSoC mode.

Acknowledgement

The authors acknowledge with gratitude the financial support provided by the Advanced Lead-Acid Battery Consortium (ALABC Project No. C2.3). We want to express our special thanks to Dr. Patrick Moseley and Dr. David Prengaman for encouraging the present investigation. This paper was reported at the ALABC Member's and Contractor's Conference 2009.

References

[1] E.J. Ritchie, Trans. Electrochem. Soc. 92 (1947) 229.
[2] T.F. Sharpe, J. Electrochem. Soc. 116 (1969) 1639.
[3] M.P.J. Brennan, N.A. Hampson, J. Electroanal. Chem. 54 (1974) 263.
[4] G. Archdale, J.A. Harrison, J. Electroanal. Chem. 48 (1973) 465.
[5] A.C. Simon, S.M. Caulder, P.J. Gurlusky, J.R. Pierson, J. Electrochem. Soc. 121 (1974) 462.
[6] B.K. Mahato, J. Electrochem. Soc. 128 (1981) 1416.
[7] D. Pavlov, S. Ignatova, J. Appl. Electrochem. 17 (1987) 715.
[8] P. Ekdunge, D. Simonsson, J. Appl. Electrochem. 19 (1989) 127.
[9] G.I. Aidman, J. Power Sources 59 (1996) 25.
[10] D.P. Boden, J. Arias, F.A. Fleming, J. Power Sources 95 (2001) 277.
[11] Y. Yamaguchi, M. Shiota, Y. Nakayama, N. Hirai, S. Hara, J. Power Sources 93 (2000) 104.
[12] B.O. Myrvold, J. Power Sources 117 (2003) 187.
[13] N. Hirai, S. Kubo, K. Magara, J. Power Sources 191 (2009) 97.
[14] K. Nakamura, M. Shiomi, K. Takahashi, M. Tsubota, J. Power Sources 59 (1996) 153.

[15] M. Shiomi, T. Funato, K. Nakamura, K. Takahashi, M. Tsubota, J. Power Sources 64 (1997) 147.
[16] A.F. Hollenkamp, W.G.A. Baldsing, S. Lau, O.V. Lim, R.H. Newnham, D.A.J. Rand, J.M. Rosalie, D.G. Vella, L.H. Vu, ALABC Project N1.2, Final Report Proceedings of Advanced Lead-Acid Battery Consortium, Research Triangle Park, NC, USA, 2002.
[17] P.T. Moseley, R.F. Nelson, A.F. Hollenkamp, J. Power Sources 157 (2006) 3.
[18] R.H. Newnham, W.G.A. Baldsing, A.F. Hollenkamp, O.V. Lim, C.G. Phyland, D.A.J. Rand, J.M. Rosalie, D.G. Vella, ALABC Project C/N1.1, Final Report Proceedings of Advanced Lead-Acid Battery Consortium, Research Triangle Park, NC, USA, 2002.
[19] M. Calabek, K. Micka, P. Krivak, P. Baca, J. Power Sources 158 (2006) 864.
[20] P.T. Moseley, J. Power Sources 191 (2009) 134.
[21] D. Pavlov, T. Rogachev, P. Nikolov, G. Petkova, J. Power Sources 191 (2009) 58.
[22] Y.B. Kasparov, E.G. Yampolskaya, B.N. Kabanov, Zh. Prikl. Khimii (J. Appl. Chem.) 37 (1964) 1936 (in Russian).
[23] G. Sterr, Electrochim. Acta 15 (1970) 1221.
[24] B.N. Kabanov, Proceedings of the 3rd Conference on Electrochemsitry, Moscow, Russia, 1953, p. 138.
[25] N.A. Hampson, J.B. Lakeman, J. Electroanal. Chem. 119 (1981) 3.
[26] D.P. Boden, J. Power Sources 73 (1998) 89.
[27] S. Ruevski, D. Pavlov, Ext. Abstr. LABAT'96 International Conference, Varna, Bulgaria, 1996, p. 46.
[28] F. Saez, B. Martinez, D. Martin, P. Spinelli, F. Trinidad, J. Power Sources 95 (2001) 174.
[29] H. Vermesan, N. Hirai, M. Shiota, T. Tanaka, J. Power Sources 133 (2004) 52.
[30] K. Sawai, T. Funato, M. Watanabe, H. Wada, K. Nakamura, M. Shiomi, S. Osumi, J. Power Sources 158 (2006) 1084.
[31] G. Petkova, D. Pavlov, J. Power Sources 113 (2003) 355.
[32] D. Pavlov, V. Iliev, J. Power Sources 7 (1981) 153.
[33] V. Iliev, D. Pavlov, J. Appl. Electrochem. 15 (1985) 39.